Search-Range-Correction-Based Doppler Shift Acquisition for Space Communications

Zhaowei Zhang, Wenchi Cheng, *Member, IEEE*, and Hailin Zhang, *Member, IEEE*

***Abstract*—For space communication circumstances, long-distance transmission significantly deteriorates the received signal-to-noise ratio (SNR) at the receiver. Moreover, the high-speed relative movement between the transmitter and the receiver causes a very large Doppler shift, thus imposing a new challenge for the acquisition. To address the Doppler shift acquisition problem under not only the very low SNR but under the very high relative movement scenarios as well, in this paper, we develop one search range correction (SRC)-based acquisition scheme, which includes three algorithms called single SRC, overlapping SRC, and iterative SRC, respectively, to significantly increase the acquisition probability for space communications. First, the single SRC algorithm, which has a simple closed-form expression for the net increment of acquisition probability, uses multiple combination periods to correct the search range for the succeeding period. Moreover, the special case using two combination periods for the single SRC algorithm is already verified to increase the acquisition probability. Second, the overlapping SRC algorithm, which is based on the period overlapping of the single SRC algorithm, enjoys much implementation feasibility and saves many received signals. Third, the iterative SRC algorithm, which builds on the iteration of the overlapping SRC algorithm, can further increase the acquisition probability as compared with that of the overlapping SRC algorithm. Simulations results show that our proposed scheme can obtain much higher acquisition probability of Doppler shift, compared with existing acquisition schemes, including the fast Fourier transform (FFT), time–frequency, and single SRC using two combination periods.**

***Index Terms*—Acquisition probability, Doppler shift acquisition, high-speed relative movement, low signal-to-noise ratio (SNR), search range correction (SRC), space communication.**

I. Introduction

As THE explorations for space environments (navigation satellites, lunar flights, and solar explorations, etc.) become increasingly active, the space communication technology [1]–[5] has attracted much attention over the past few decades. Under the space communication scenarios, there are some specific challenges that would not be encountered in wireless communications on Earth. First, the limited transmission power on the space terminals and the extremely long distance between the transmitter and receiver are likely to result in very low received signal-to-noise ratio (SNR) signals, which are completely buried in the large background noise and are very hard to detect [2]–[4]. Second, the universe planet's gravitational force, Earth's rotation, and relatively high-speed movement between the transmitter–receiver pair in space environments cause a very large Doppler shift (with magnitude at 0.1 MHz or even 1 MHz) on the carrier frequency [5], [6], which seriously degrades the carrier synchronization for signal recovery at the receiver. Moreover, when the relative velocity between the transmitter and receiver varies fast with time, there also exists a very large acceleration for dynamic Doppler shift. Under large acceleration scenarios, the dynamic Doppler shift even drifts over a very wide frequency range.

It is necessary to compensate the Doppler shift on carrier frequency to remove the impact of frequency shift on the signal recovery at the receiver. The existing works focus on how to accurately acquire the Doppler shift value from the received signals [7]–[13], which refers to the Doppler shift acquisition problem. An expectation–maximization based adaptive estimation method is proposed in [8] to obtain the accurate Doppler shift. By exploiting the sparsity of signal, a two-stage deterministic compressed acquisition technique is presented in [9], which is based on the compressed sensing principle. In [10] satellite orbit parameters and ground station position were used to develop the Doppler shift acquisition scheme. However, the fast Fourier transform (FFT)-based acquisition methods [11]–[13], which significantly accelerate the acquisition process over a wide range of frequency-shift offsets with low complexity, have attracted much attention among existing Doppler shift acquisition schemes. The generic model of discrete Fourier transform processing for the single parameter estimation is given in [11]. Based on the FFT method, the fast acquisition of the Doppler shift for the direct-sequence spread spectrum (DSSS) signals with a large Doppler shift offset is addressed for both the low-Earth-orbit satellite communications [12] and global position systems [13].

First, under very low SNR scenarios, the FFT over only one received symbol period cannot provide the sufficiently high output SNR for a reliable acquisition. To obtain the high output SNR [13]–[15], a number of received symbols need to be coherently, noncoherently, or differentially combined to accumulate the signal energy in one combination period. However, the Doppler shift acquisition schemes in [13]–[15] only

Manuscript received June 26, 2014; revised April 1, 2015; accepted April 21, 2015. Date of publication May 12, 2015; date of current version May 12, 2016. This work was supported in part by the National Natural Science Foundation of China under Grant 61401330, Grant 61371127, and Grant 61301169; by the 111 Project of China under Grant B08038; and by the Fundamental Research Funds for the Central Universities under Grant 7214603701. The review of this paper was coordinated by Dr. T. Jiang.

The authors are with the State Key Laboratory of Integrated Service Networks, Xidian University, Xi'an 710071, China (e-mail: zwzhang2012@hotmail.com; wccheng@xidian.edu.cn; hlzhang@xidian.edu.cn).

Color versions of one or more of the figures in this paper are available online at http://ieeexplore.ieee.org.

Digital Object Identifier 10.1109/TVT.2015.2432456

consider the constant Doppler shift without taking into account the impact of acceleration on the acquisition performance. Second, under the large acceleration scenarios, the dynamic Doppler shift varies very fast over a wide frequency range, thus causing the serious energy dispersion problem [16]–[20] during the combination stage. In [16], the impact of acceleration on the acquisition probability is analyzed. However, they do not give solutions to this problem. A straight-line approximation is proposed in [19] to remove the acceleration's impact, only for small acceleration cases. The time–frequency method [17], [18], which shows the variation of Doppler shift with time, can detect the accelerating targets. However, this method needs a very high SNR. A framework for acceleration compensation and step sizes for full or partial compensation is developed in [20] to mitigate the Doppler shift migration. However, the computation complexity of acceleration compensation significantly increases as the acceleration increases, Therefore, the aforementioned schemes cannot thoroughly solve the serious energy dispersion problem under not only a very low SNR but in very large acceleration scenarios as well.

In views of that the maximum likelihood (ML) estimation for the Doppler shift is equivalent to the spectrum peak search on the FFT, there comes a series of improved schemes [21]–[26]. One is the two-step search strategy [22], [23]. For instance, the proposed search algorithm in [22] consists of two steps, i.e., coarse search and fine search for the periodogram peak, which can be conducted in a narrower frequency range. The other is the iterative search strategy [24]–[26]. In [24], an iterative dichotomous search algorithm was presented for the real signal frequency by confining the estimation result into a gradually narrower search range, whereas in [25], a modified dichotomous search estimator was proposed, which operates on the unpadded data sequence. Although the mentioned schemes in [22]–[26], which concentrate on the acquisition accuracy, are based on the high SNR constraint, the idea of narrowing the search range for spectrum peak search is of great inspiration.

To address the energy dispersion problem under not only the very low SNR constraint but also the very large acceleration constraint, our preliminary research [27] shows that the single search range correction (SRC) algorithm using two combination periods confines the Doppler shift estimation into a very accurate search range and increases the detection probability. However, it does not discuss the scenario using multiple combination periods and does not show the optimal number of combination periods. In this paper, we develop one SRC-based acquisition scheme, including three algorithms, which are called single SRC, overlapping SRC, and iterative SRC, to significantly increase the acquisition probability for space communications. Although the single SRC algorithm using two combination periods is already verified to significantly increase the acquisition probability for the highly dynamic Doppler shift, the generic single SRC algorithm proposed in the paper uses multiple combination periods and shows the optimal number of combination periods. The overlapping SRC algorithm, which is based on the period overlapping of single SRC not only increases much implementation feasibility but saves many received signals as well. The iterative SRC algorithm, which builds on the iterative of overlapping SRC, can further increase the acquisition probability, as compared with the overlapping SRC algorithm.

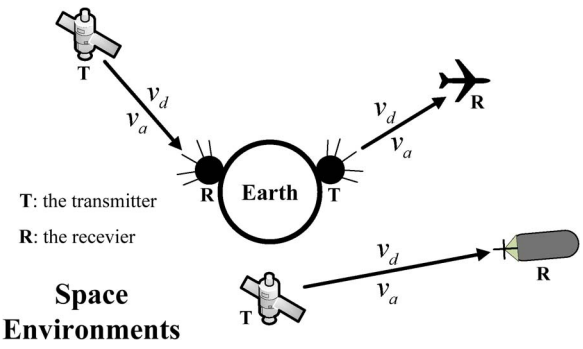

Fig. 1. System model.

The reminder of this paper is organized as follows. Section II introduces the system model and formulates the acquisition problem for the transmitter–receiver pairs in space communications. In Section III, we develop the SRC-based acquisition scheme, including the single SRC, the overlapping SRC, and the iterative SRC, respectively, to increase the acquisition probability, followed by the simulation results given in Section IV to evaluate our developed acquisition scheme for space communication scenarios. Section V concludes this paper.

II. System Model and Problem Formulation

We consider the generic communication transmission model for a highly moving transmitter–receiver pair in the space scenarios, with a large relative radial velocity v_d and acceleration v_a, which is shown in Fig. 1.

High-speed relative movement between the transmitter and receiver causes a large Doppler shift f_d on the carrier frequency. Moreover, when the relative velocity between the transmitter–receiver pair varies fast with time, there exists a large acceleration f_a. Then, f_d and f_a are given by

$$f_d = \frac{v_d}{v_c} f_c, \quad f_a = \frac{v_a}{v_c} f_c \tag{1}$$

where $v_c = 3 \times 10^8$ m/s is the speed of light, and f_c is the carrier frequency used in space communications. Consequently, the signal frequency linearly varies with time t as $f_d + f_a t$, and the signal phase can be further derived as $2\pi \int_0^t (f_d + f_a \tau) d\tau = 2\pi(f_d t + 0.5 f_a t^2)$. Then, after discrete sampling (i.e., $t = n/f_s$), the received signal during one symbol period is denoted by $\boldsymbol{x} = [x_0, \ldots, x_{N-1}]$, where the element x_n of $\boldsymbol{x}$ can be derived as follows:

$$x_n = abe^{j\left[2\pi\left(\frac{f_d}{f_s}n + \frac{f_a}{2f_s^2}n^2\right) + \varphi_0\right]} + w_n, \quad n = 0, \ldots, N-1 \tag{2}$$

where a is the symbol amplitude, $b \in \{-1, +1\}$ is an unknown sign with the bit rate r_b, f_s is the sampling rate, φ_0 is the initial phase, and w_n is an additive complex white zero-mean Gaussian noise with variance σ^2 Then, we have the length of one symbol vector as $N = f_s/r_b$.

The large and dynamic Doppler shift between the transmitter and the receiver causes a huge SNR loss at the receiver, thus greatly distorting the signal recovery. Hence, the receiver needs to compensate the Doppler shift on the carrier frequency, during which how to accurately acquire the Doppler shift value from the received signals becomes the core issue. Let $\mathrm{FFT}(\boldsymbol{x})$ denote the N_f point $(N_f \geq N)$ complex FFT on $\boldsymbol{x}$. Based on the ML detection (i.e., spectrum peak search) [28], we can derive the estimation $\widehat{f}_d$ for Doppler shift as

$$\widehat{f}_d = \frac{\arg\max |\mathrm{FFT}(\boldsymbol{x})|}{N_f} f_s \tag{3}$$

where $\arg\max |\mathrm{FFT}(\boldsymbol{x})|$ indicates the location of spectrum peak on vector $|\mathrm{FFT}(\boldsymbol{x})|$.

Under the very low SNR caused by the serious path loss over the long-distance transmission in space communication scenarios, the spectrum peak on the FFT over only one received symbol period is completely buried in the large background noise and is very hard to detect. To obtain a higher output SNR at the receiver for a reliable estimation, we need to combine a number of received symbols to accumulate the signal energy. Because the transmitted symbol sign $(b \in \{-1, +1\})$ is unknown to the receiver, we adopt the noncoherent combination policy [14]. Then, the combination result $\boldsymbol{I}_c$ during the combination period is given by

$$\boldsymbol{I}_c = \sum_{i=1}^{L_c} \left| \boldsymbol{I}^{[i]} \right| = \sum_{i=1}^{L_c} \left| \mathrm{FFT}(\boldsymbol{x}^{[i]}) \right| \tag{4}$$

where $\boldsymbol{I}^{[i]} = \mathrm{FFT}(\boldsymbol{x}^{[i]})$ is the FFT over the ith received symbol $\boldsymbol{x}^{[i]}$, and L_c is called the combination length (i.e., the total number of symbols combined in one combination period).

However, due to the existence of acceleration, the output SNR is the concave function with respect to the combination length L_c. This is because the dynamic Doppler shift causes the serious energy dispersion problem that greatly mitigates the signal energy accumulation. We denote the optimal combination length of L_c by L_{opt}, which corresponds to the maximum output SNR. The parameter L_{opt} only relates with f_a and has the empirical expression given by $L_{\mathrm{opt}} \simeq 10^{0.5606}(2\pi f_a / f_s^2)^{-0.5}$ [16]. Furthermore, because the larger acceleration leads to the wider energy dispersion in the combination period, L_{opt} monotonically decreases as f_a increases.

The two constraints given cause the conflict that the low SNR requires a long combination period to accumulate the signal energy while the large acceleration limits the combination length, although there are much more received symbols available. Thus, there comes the very challenging problem: how to efficiently acquire the Doppler shift under not only the very low SNR but also the very large acceleration scenarios in space communications.

In this paper, we develop one novel Doppler shift acquisition scheme to efficiently solve this challenging but critical problem for space communications.

III. Proposed Search Range Correction Scheme

The Nyquist sampling theorem requires that the sampling frequency f_s needs to be no less than two times the maximum Doppler shift $F_{\max}$. Thus, we have

$$f_s \geq 2F_{\max} = 2v_{\max} f_c / v_c \tag{5}$$

where $F_{\max} = v_{\max} f_c / v_c$ is determined by the largest relative velocity $v_{\max}$ between the transmitter–receiver pair. Then, the Doppler shift falls into the frequency range $R = [-F_{\max}, F_{\max}]$, which clearly satisfies $R \subseteq [-f_s/2, f_s/2]$.

We use $(M+1)L_{\mathrm{opt}}(M \geq 2)$ successive received symbols to construct $(M+1)$ combination periods. Based on the noncoherent combination policy in each combination period, we can obtain $\{\boldsymbol{I}_c^{[1]}, \ldots, \boldsymbol{I}_c^{[M+1]}\}$, where $\boldsymbol{I}_c^{[t]} (1 \leq t \leq M+1)$ is the combination result derived in the tth period and given by

$$\boldsymbol{I}_c^{[t]} = \sum_{i=1+(t-1)L_{\mathrm{opt}}}^{tL_{\mathrm{opt}}} |\boldsymbol{I}^{[i]}|. \tag{6}$$

Thus, the spectrum peak search (i.e., ML detection) problem in the tth combination period can be formulated as follows:

$$y^{[t]} = \arg\max \boldsymbol{I}_c^{[t]} \tag{7}$$

$$\text{s.t.} : y^{[t]} f_s / N_f \in R \tag{8}$$

where (8), which is called the search range constraint, confines the spectrum peak search into the search range $R = [-F_{\max}, F_{\max}]$.

For $1 \leq t \leq M$, by substituting $\boldsymbol{I}_c^{[t]}$ specified in (6) and R into (7) and (8), respectively, we can obtain $y^{[t]}$ and then derive the acquisition result $\widehat{f}_d(t) = y^{[t]} f_s / N_f \in R$ in the tth combination period. To evaluate the acquisition performance, we assume $\widehat{f}_d(t)$ is true if it satisfies

$$\widehat{f}_d(t) \in [f_d(t) - \theta, f_d(t) + \theta] \tag{9}$$

where $f_d(t)$ is the median value of Doppler shift during the tth combination period, and θ is a tolerable threshold for acquisition.

From the perspective of search range, the spectrum peak search in (3) is conducted in the frequency range $[-f_s/2, f_s/2]$, which is determined by the sampling frequency f_s. The largest velocity $v_{\max}$ implies that the Doppler shift falls into the frequency range R and then confines the spectrum peak search into the smaller but more accurate search range R, as compared with $[-f_s/2, f_s/2]$. Clearly, it can be expected that a more accurate search range is beneficial for the higher acquisition performance.

In this paper, we develop the SRC-based acquisition scheme to further confine the spectrum peak search into a much more accurate search range than the search range R, thus significantly increasing the acquisition probability for space communications. Our developed scheme includes three algorithms, which are called single SRC, overlapping SRC, and iterative SRC, respectively.

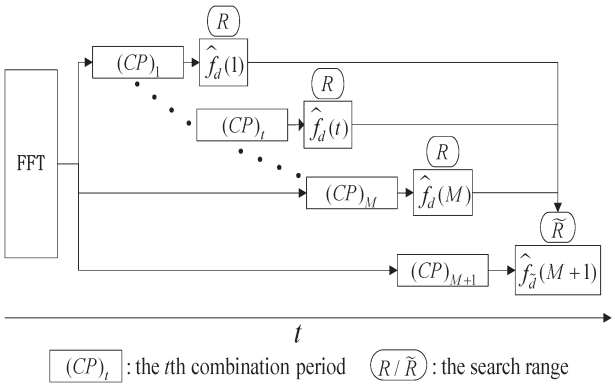

Fig. 2. Single SRC algorithm.

A. Single SRC Algorithm

Let T_s denote the duration time during one symbol period, then $T_s = 1/r_b$. The Doppler shift varies fast with time, but its variation rate is limited by the acceleration v_a. In other words, the maximum drift of Doppler shift over one received symbol period, which is denoted by δ_s, is given by

$$\delta_s = f_a T_s = \frac{v_a f_c}{v_c r_b}. \tag{10}$$

In the single SRC algorithm, the acquisition results derived in the first M combination periods are used to correct the search range for the acquisition in the $(M+1)$th combination period. The single SRC algorithm is shown in Fig. 2.

Based on the drift of Doppler shift from the first to the $(M+1)$th combination period, we propose the new search range, which is denoted by $\widetilde{R}$, for the $(M+1)$th acquisition, which is defined as follows:

$$\widetilde{R} = \Big[\max\{\widehat{f}_{\min} - M\delta_c - 2\theta, -F_{\max}\} \quad \min\{\widehat{f}_{\max} + M\delta_c + 2\theta, F_{\max}\}\Big] \tag{11}$$

where $\widehat{f}_{\min} = \min\{\widehat{f}_d(1), \ldots, \widehat{f}_d(M)\}$ denotes the minimum one in $\{\widehat{f}_d(1), \ldots, \widehat{f}_d(M)\}$, $\widehat{f}_{\max} = \max\{\widehat{f}_d(1), \ldots, \widehat{f}_d(M)\}$ denotes the maximum one among $\{\widehat{f}_d(1), \ldots, \widehat{f}_d(M)\}$, and $\delta_c = L_{\text{opt}}\delta_s$ is the drift of the Doppler shift during one combination period.

To compare the search range $\widetilde{R}$ with R, we will show the relationship between $f_d(M+1)$, $\widetilde{R}$, and R in Theorem 1.

Theorem 1: If the acquisition results $\{\widehat{f}_d(1), \ldots, \widehat{f}_d(M)\}$ derived in the first M combination periods satisfy any one of the following two conditions.

1) There exists at least one true acquisition result.
2) They are all false but there exist two integers $\lambda_1, \lambda_2 \in [1, M]$ such that $(\widehat{f}_d(\lambda_1) - f_d(M+1))(\widehat{f}_d(\lambda_2) - f_d(M+1)) \le 0$; then, we have

$$f_d(M+1) \in \widetilde{R} \subseteq R. \tag{12}$$

Proof: We will prove Theorem 1 by verifying each of the two conditions in Cases 1 and 2, respectively.

Case 1: Suppose the acquisition result $\widehat{f}_d(i)$ derived in the ith $(1 \le i \le M)$ combination period is true. From (9), we have $|\widehat{f}_d(i) - f_d(i)| \le \theta$.

If the transmitter/receiver keeps accelerating from the ith to the $(M+1)$th combination period, there exists the largest drift of Doppler shift as

$$|f_d(i) - f_d(M+1)| \le (M+1-i)\delta_c. \tag{13}$$

Based on the acquisition result $\widehat{f}_d(i)$, we can obtain the location of $f_d(M+1)$ in the $(M+1)$th combination period as follows:

$$f_d(M+1) \in \Big[\max\Big\{\widehat{f}_d(i) - (M+1-i)\delta_c - 2\theta, -F_{\max}\Big\} \quad \min\Big\{\widehat{f}_d(i) + (M+1-i)\delta_c + 2\theta, F_{\max}\Big\}\Big]. \tag{14}$$

Because of $\widehat{f}_{\min} \le \widehat{f}_d(i) \le \widehat{f}_{\max}$ and $(M+1-i) \le M$, it can be clearly derived that

$$\widehat{f}_d(i) - (M+1-i)\delta_c - 2\theta \ge \widehat{f}_{\min} - M\delta_c - 2\theta \tag{15}$$

$$\widehat{f}_d(i) + (M+1-i)\delta_c + 2\theta \le \widehat{f}_{\max} + M\delta_c + 2\theta. \tag{16}$$

By substituting (15) and (16) into (14), we can further have $f_d(M+1) \in \widetilde{R}$.

Case 2: Suppose $\widehat{f}_d(\lambda_1) \le f_d(M+1)$ and $\widehat{f}_d(\lambda_2) \ge f_d(M+1)$, then we have

$$f_d(M+1) \in \Big[\max\Big\{\widehat{f}_d(\lambda_1) - \theta, -F_{\max}\Big\} \quad \min\Big\{\widehat{f}_d(\lambda_2) + \theta, F_{\max}\Big\}\Big]. \tag{17}$$

Due to $\widehat{f}_{\min} \le \widehat{f}_d(\lambda_1) \le \widehat{f}_d(\lambda_2) \le \widehat{f}_{\max}$, clearly, we can obtain $\widehat{f}_d(\lambda_1) - \theta \ge \widehat{f}_{\min} - M\delta_c - 2\theta$ and $\widehat{f}_d(\lambda_2) + \theta \le \widehat{f}_{\max} + M\delta_c + 2\theta$, which imply that $f_d(M+1) \in \widetilde{R}$. Similarly, if $\widehat{f}_d(\lambda_1) \ge f_d(M+1)$ and $\widehat{f}_d(\lambda_2) \le f_d(M+1)$, $f_d(M+1) \in \widetilde{R}$ still holds.

From the conclusions in Cases 1 and 2, $f_d(M+1) \in \widetilde{R}$ always holds. In addition, since we have $\max\{\widehat{f}_{\min} - M\delta_c - 2\theta, -F_{\max}\} \ge -F_{\max}$, and $\min\{\widehat{f}_{\max} + M\delta_c + 2\theta, F_{\max}\} \le F_{\max}$, we can obtain $\widetilde{R} \subseteq R$. Thus, Theorem 1 follows. ■

From Theorem 1, we can observe that, unless all the M acquisition results derived in the first M combination periods are false and they are larger or smaller than $f_d(M+1)$, $f_d(M+1) \in \widetilde{R}$ always holds. This means the $(M+1)$th spectrum peak search can be confined into the smaller but more accurate range $\widetilde{R}$.

By substituting $\boldsymbol{I}_c^{[M+1]}$ and this new search range $\widetilde{R}$ into (7) and (8), respectively, we can obtain $\widetilde{y}^{[M+1]}$ and then derive the

acquisition result $\widehat{f}_{\widetilde{d}}(M+1)$ as follows:

$$\widehat{f}_{\widetilde{d}}(M+1) = \frac{\widetilde{y}^{[M+1]} f_s}{N_f} \in \widetilde{R} \tag{18}$$

which implies that the $(M+1)$th acquisition result $\widehat{f}_{\widetilde{d}}(M+1)$ falls into the smaller and more accurate search range $\widetilde{R}$, as compared with $\widehat{f}_d(t)$ $(1 \le t \le M)$.

To compare $\widehat{f}_{\widetilde{d}}(M+1)$ with $\widehat{f}_d(M+1)$,[1] we define $\widetilde{\eta}$ as the increase of acquisition probability for the case that $\widehat{f}_d(M+1)$ is false but $\widehat{f}_{\widetilde{d}}(M+1)$ is true. We also define η as the decrease in acquisition probability for the case that $\widehat{f}_d(M+1)$ is true but $\widehat{f}_{\widetilde{d}}(M+1)$ is false. Let p denote the acquisition probability for $\widehat{f}_d(t)$ $(1 \le t \le M)$. Clearly, the acquisition probability for $\widehat{f}_d(M+1)$ is also p. Then, we calculate η and $\widetilde{\eta}$ using Theorem 2 under the condition that $f_d(M+1) \in \widetilde{R} \subseteq R$.

Theorem 2: If $f_d(M+1)$ satisfies $f_d(M+1) \in \widetilde{R} \subseteq R$, then we have

$$\begin{cases} \eta = 0 \\ \widetilde{\eta} = p^{\gamma} - p \ge 0 \end{cases} \tag{19}$$

where $\gamma = (\widetilde{D} - 2\theta)/(2F_{\max} - 2\theta)$, and $\widetilde{D} = (\min\{\widehat{f}_{\max} + M\delta_c + 2\theta, F_{\max}\} - \max\{\widehat{f}_{\min} - M\delta_c - 2\theta, -F_{\max}\})$ denotes the length of search range $\widetilde{R}$.

Proof: For convenience of description, we divide all the N_f elements of $\boldsymbol{I}_c^{[M+1]}$ into two categories: the signal category that consists of the elements falling into the tolerable range $[f_d(M+1) - \theta, f_d(M+1) + \theta]$, and the noise category that consists of the remaining elements.

Let N_I denote the total number of noise elements located in the search range R, then we have $N_I = (2F_{\max} - 2\theta)N_f/f_s$. Correspondingly, the element set $\boldsymbol{\nu}$ used for the spectrum peak search in R can be derived as

$$\boldsymbol{\nu} = \{\nu_1, \ldots, \nu_i, \nu_s, \nu_{i+1}, \ldots, \nu_{N_I}\} \tag{20}$$

where $\nu_i \in \boldsymbol{I}_c^{[M+1]}$ $(1 \le i \le N_I)$ is the ith noise element, and ν_s denotes the largest signal element. Based on the ML estimation in the search range R, the acquisition probability p for the acquisition result $\widehat{f}_d(M+1)$ can be given by

$$p = \Pr\{\nu_{\max} < \nu_s\} \tag{21}$$

where $\nu_{\max} = \max\{\boldsymbol{\nu} \setminus \{\nu_s\}\} = \max\{\nu_1, \ldots, \nu_{N_I}\}$ denotes the largest noise element.

Suppose all the noise elements are independent and identically distributed (i.i.d.) with a cumulative distribution function (cdf) [29] denoted by $G(\lambda)$, where λ denotes the value of noise element. Since the cdf of $\nu_{\max}$ can be derived as $\Pr\{\nu_{\max} < \lambda\} = [G(\lambda)]^{N_I}$, we can rewrite the acquisition probability p as

$$p = [G(\nu_s)]^{N_I}. \tag{22}$$

In the similar way, the acquisition probability q[2] in the search range $\widetilde{R}$ can be given by

$$q = [G(\nu_s)]^{\widetilde{N}_I} \tag{23}$$

where $\widetilde{N}_I = (\widetilde{D} - 2\theta)N_f/f_s$ denotes the total number of noise elements in the search range $\widetilde{R}$. From (22) and (23), the relationship between p and q can be expressed as

$$q = p^{\frac{\widetilde{N}_I}{N_I}} = p^{\frac{(\widetilde{D}-2\theta)}{(2F_{\max}-2\theta)}} = p^{\gamma}. \tag{24}$$

Equation (24) shows that the acquisition probability q, which can also be denoted by $q(\widetilde{D})$, is a function with respect to $\widetilde{D}$. Due to $0 < p < 1$, we have

$$\frac{\partial q(\widetilde{D})}{\partial \widetilde{D}} = \frac{q \ln p}{2F_{\max} - 2\theta} < 0 \tag{25}$$

which indicates that q monotonically decreases as $\widetilde{D}$ increases. From the denotation of $\widetilde{D}$, clearly, we can obtain that $\widetilde{D} \le 2F_{\max}$, which verifies $q \ge q(2F_{\max}) = p$.

Because of $\widetilde{R} \subseteq R$, we have $\widetilde{\nu}_{\max} \le \nu_{\max}$, where $\widetilde{\nu}_{\max}$ is the largest noise element in the search range $\widetilde{R}$. If $\widehat{f}_d(M+1)$ is true (i.e., $\nu_s > \nu_{\max}$), then we have

$$\nu_s > \nu_{\max} \ge \widetilde{\nu}_{\max} \tag{26}$$

which implies that $\widehat{f}_{\widetilde{d}}(M+1)$ must also be true. This means that $\eta = 0$ always holds. Then, we can obtain $\widetilde{\eta}$ as follows:

$$\widetilde{\eta} = q - p = p^{\gamma} - p \ge 0. \tag{27}$$

Thus, Theorem 2 follows. ■

From Theorem 2, only if $f_d(M+1) \notin \widetilde{R}$ holds, η can be not equal to 0, which makes $\widehat{f}_{\widetilde{d}}(M+1)$ false although $\widehat{f}_d(M+1)$ is true. It can be further derived from Theorem 1 that only if all the first M acquisitions in $\{\widehat{f}_d(1), \ldots, \widehat{f}_d(M)\}$ are false and they are smaller or larger than $f_d(M+1)$ can $f_d(M+1) \notin \widetilde{R}$ hold.

To obtain the net increment $\Delta\eta$ (i.e., $\Delta\eta = \widetilde{\eta} - \eta$) of acquisition probability, without loss of generality, we assume that $f_d(M+1)$ is uniformly distributed in the search range R. Based on all possible cases of $\{\widehat{f}_d(1), \ldots, \widehat{f}_d(M)\}$, we will derive η and $\widetilde{\eta}$, with the emphasis on solution of $\widetilde{D}$, which is given in Theorem 2.

In the real-world situation, one cannot know whether one acquisition result is true or false. Hence, we have to take

[1] $\widehat{f}_d(M+1)$ is obtained by substituting $\boldsymbol{I}_c^{[M+1]}$ and R into (7) and (8), respectively, to compare with $\widehat{f}_{\widetilde{d}}(M+1)$ to show the impact of search range on acquisition probability.

[2] Note that the acquisition probability q in (23) is not equal to the acquisition probability for $\widehat{f}_{\widetilde{d}}(M+1)$ because q is derived based on the condition that $f_d(M+1) \in \widetilde{R} \subseteq R$. Because we cannot know whether $\widehat{f}_d(t)$ $(1 \le t \le M)$ is true or false, there still exists another case in which $f_d(M+1) \notin \widetilde{R}$.

all possible cases of $\{\widehat{f}_d(1),\ldots,\widehat{f}_d(M)\}$ into consideration. Let m denote the total number of false acquisitions in $\{\widehat{f}_d(1),\ldots,\widehat{f}_d(M)\}$; then, we have the following three cases.

Case I $(m=0)$*:* All acquisition results in $\{\widehat{f}_d(1),\ldots,\widehat{f}_d(M)\}$ are false, with the probability p^M. Clearly, $f_d(M+1)\in\widetilde{R}$ holds in this case. Then, based on (11), we can obtain the length of search range $\widetilde{R}$ as $\widetilde{D}_0=(3M-1)\delta_c+4\theta$.[3] Thus, from Theorem 2, η_0 and $\widetilde{\eta}_0$ can be derived as follows:

$$\begin{cases}\eta_0=0\\ \widetilde{\eta}_0=p^M(p^{\gamma_0}-p)\end{cases}\tag{28}$$

where $\gamma_0=(\widetilde{D}_0-2\theta)/(2F_{\max}-2\theta)$.

Case II $(1\le m\le M-1)$*:* There are m false acquisitions in $\{\widehat{f}_d(1),\ldots,\widehat{f}_d(M)\}$, with the probability $C_m^M p^{M-m}(1-p)^m$. In this case, $f_d(M+1)\in\widetilde{R}$ also holds.

Due to the influence of random noise, all these m false acquisitions are i.i.d. with an identical cumulative distribution function (cdf) [29], which is given by

$$Z(\lambda)=\frac{\lambda+F_{\max}}{2F_{\max}},\quad -F_{\max}\le\lambda\le F_{\max}\tag{29}$$

where λ denotes the value of false acquisition.

Let $\{e_1,\ldots,e_m\}$ denote the set of m false acquisitions where $e_i\in\{\widehat{f}_d(1),\ldots,\widehat{f}_d(M)\}$ $(1\le i\le m)$. The cdfs of $e_{\max}$ and $e_{\min}$ can be derived as $Z_{\max}(\lambda)=[Z(\lambda)]^m$ and $Z_{\min}(\lambda)=1-[1-Z(\lambda)]^m$, respectively, where $e_{\max}=\max\{e_1,\ldots,e_m\}$ and $e_{\min}=\min\{e_1,\ldots,e_m\}$. Thus, the average values $\overline{E}_m$ for $e_{\max}$ and $\underline{E}_m$ for $e_{\min}$ can be derived as follows:

$$\begin{aligned}\overline{E}_m&=\int_{-F_{\max}}^{F_{\max}}\lambda dZ_{\max}(\lambda)\\ &=\lambda\left(\frac{\lambda+F_{\max}}{2F_{\max}}\right)^m\Big|_{-F_{\max}}^{F_{\max}}-\int_{-F_{\max}}^{F_{\max}}\left(\frac{\lambda+F_{\max}}{2F_{\max}}\right)^m d\lambda\\ &=\left(1-\frac{2}{m+1}\right)F_{\max}\end{aligned}\tag{30}$$

$$\underline{E}_m=\int_{-F_{\max}}^{F_{\max}}\lambda dZ_{\min}(\lambda)=-\overline{E}_m.\tag{31}$$

From (30) and (31), we can observe that the average $\overline{E}_m$ for $e_{\max}$ becomes closer to $F_{\max}$ as m increases. Similarly, the average $\underline{E}_m$ for $e_{\min}$ becomes closer to $-F_{\max}$ as m increases. Consequently, by the integration over the range $[-F_{\max},F_{\max}]$, we can obtain the length of search range $\widetilde{R}$ (denoted by $\widetilde{D}_m$) as follows:

$$\begin{aligned}\widetilde{D}_m=\frac{1}{2F_{\max}}&\left(\int_{-F_{\max}}^{\underline{E}_m}\left[\overline{E}_m+2(M\delta_c+2\theta)-\lambda\right]d\lambda\right.\\ &+\int_{\underline{E}_m}^{\overline{E}_m}\left[\overline{E}_m+2(M\delta_c+2\theta)-\underline{E}_m\right]d\lambda\\ &\left.+\int_{\overline{E}_m}^{F_{\max}}\left[\lambda+2(M\delta_c+2\theta)-\underline{E}_m\right]d\lambda\right)\\ =&-\frac{1}{2}(\lambda-\overline{E}_m)^2\Big|_{-F_{\max}}^{F_{\max}}+\lambda(\overline{E}_m-\underline{E}_m)^2\Big|_{-F_{\max}}^{F_{\max}}\\ &+\frac{1}{2}(\lambda-\underline{E}_m)^2\Big|_{-F_{\max}}^{F_{\max}}+2(M\delta_c+2\theta)\\ =&2\left(\frac{m}{m+1}\right)^2F_{\max}+2(M\delta_c+2\theta).\end{aligned}\tag{32}$$

Then, from Theorem 2, η_m and $\widetilde{\eta}_m$ can be derived as

$$\begin{cases}\eta_m=0\\ \widetilde{\eta}_m=C_m^Mp^{M-m}(1-p)^m(p^{\gamma_m}-p)\end{cases}\tag{33}$$

where $\gamma_m=(\widetilde{D}_m-2\theta)/(2F_{\max}-2\theta)$.

Case III $(m=M)$*:* All the first M acquisitions are false, with the probability $(1-p)^M$. Substituting $m=M$ into (30) and (31), we can obtain $\overline{E}_M$ and $\underline{E}_M$. Clearly, the length of search range $\widetilde{R}$ can be given by $\widetilde{D}_M=\overline{E}_M-\underline{E}_M+2(M\delta_c+2\theta)=2(M-2)F_{\max}/M+2(M\delta_c+2\theta)$.

According to the location of $f_d(M+1)$ in the search range $R=[-F_{\max},F_{\max}]$, there are two subcases, as follows.

Case III-A: If $f_d(M+1)\in\widetilde{R}$, with the probability as $\widetilde{D}_M/(2F_{\max})$ (because $f_d(M+1)$ is assumed uniformly distributed in R), $\widetilde{\eta}_M$ can be given by

$$\widetilde{\eta}_M=\frac{\widetilde{D}_M}{2F_{\max}}(1-p)^M(p^{\gamma_M}-p)\tag{34}$$

where $\gamma_M=(\widetilde{D}_M-2\theta)/(2F_{\max}-2\theta)$.

Case III-B: If $f_d(M+1)\notin\widetilde{R}$, with the probability $1-\widetilde{D}_M/(2F_{\max})$, η_M is given by

$$\eta_M=\left(1-\frac{\widetilde{D}_M}{2F_{\max}}\right)(1-p)^Mp.\tag{35}$$

From **Case I** $(m=0)$, **Case II** $(1\le m\le M-1)$, and **Case III** $(m=M)$, we can obtain the net increment $\triangle\eta$ of acquisition probability as follows:

$$\triangle\eta=\sum_{m=0}^{M}(\widetilde{\eta}_m-\eta_m)=\sum_{m=0}^{M}\widetilde{\eta}_m-\eta_M.\tag{36}$$

[3]Here, $\widetilde{D}_m$, γ_m, η_m, and $\widetilde{\eta}_m$ $(0\le m\le M)$ are employed to denote $\widetilde{D}$, γ, η, and $\widetilde{\eta}$ (given in Theorem 2) under Cases 1–3, where the subscript m denotes the index.

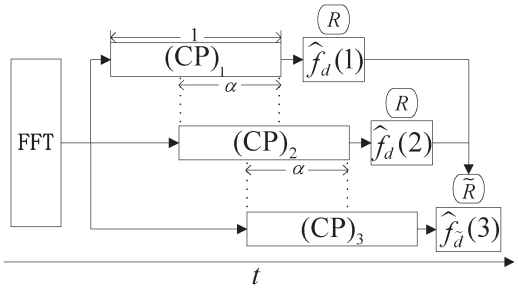

Fig. 3. Overlapping SRC algorithm.

The acquisition probability p for $\widehat{f}_d(M+1)$ is derived in search range R, whereas the acquisition probability $\widetilde{p}$ for $\widehat{f}_{\widetilde{d}}(M+1)$ is derived in a more accurate search range $\widetilde{R}$. Hence, the single SRC algorithm results in the acquisition probability increase from p to $\widetilde{p} = p + \Delta\eta$.

Equation (36) shows that the net increment $\triangle\eta$ (can be also written as $\triangle\eta(M)$) of acquisition probability corresponds to the value of M. When M increases, η_M decreases due to $\partial\widetilde{D}_M/\partial M > 0$, but $\widetilde{\eta}_m$ $(1 \le m \le M)$ also decreases. To obtain the largest value for the net increment $\Delta\eta(M)$, we need to choose an optimal M^* by solving such an optimization problem [30] as follows:

$$M^* = \arg\max_{M\ge 2} \triangle\eta(M). \tag{37}$$

By the derivation of $\triangle\eta(M)$ with M, we can find that $\partial\triangle\eta(M)/\partial M < 0$, which means that $\triangle\eta(M)$ monotonically decreases as M increases. As a result, $M^* = 2$ is the optimal solution for the single SRC algorithm, which also explains why $M = 2$ is chosen in [27].

The single SRC algorithm described in Section III-A reflects the core idea of narrowing the search range for spectrum peak search. Based on the single SRC algorithm, we will reinforce it in such two directions: the overlapping and the iterative, respectively; see Section III-B and C.

B. Overlapping SRC Algorithm

The single SRC algorithm enhances the acquisition probability by using multiple combination periods to confine the spectrum peak search into a smaller but more accurate search range. However, it also has two limitations: 1) the combination length in each combination period is constant and unchangeable; and 2) it requires at least three times received symbols, thus causing a much longer acquisition time. To overcome the limitations of the single SRC algorithm, we propose the overlapping SRC algorithm, which is shown in Fig. 3.

To explain the overlapping policy in the overlapping SRC algorithm, we define the overlapping factor α in Definition 1.

Definition 1: Let $\boldsymbol{a} = [a_1, \ldots, a_l]$ and $\boldsymbol{b} = [b_1, \ldots, b_l]$ denote two $1 \times l$ vectors. If there exist three integers $l_1, l_2, l_c \in [1, l]$ such that $[a_{l_1}, \ldots, a_{l_1+l_c-1}] = [b_{l_2}, \ldots, b_{l_2+l_c-1}]$, then $\alpha = l_c/l$ is defined as the overlapping factor.

It is also particularly noted that $\alpha = 0$ is defined to represent no overlapping.

Let $\boldsymbol{X} = [\boldsymbol{x}^{[1]}, \ldots, \boldsymbol{x}^{[L]}]$ denote the set of the received symbols available at the receiver, where L (maybe larger or smaller than $3L_{\rm opt}$) is the total number of these symbols. Similar to the single SRC algorithm described in Section III-A, we also divide $\boldsymbol{X}$ into three successive combination periods, denoted by $\boldsymbol{X}_t = [\boldsymbol{X}_{t,1}, \ldots, \boldsymbol{X}_{t,i}, \ldots, \boldsymbol{X}_{t,l_{\rm sub}}]$ $(1 \le t \le 3$ and $1 \le i \le l_{\rm sub})$ where $\boldsymbol{X}_{t,i}$ denotes the ith received symbol in the tth combination period, and $l_{\rm sub}$ is the combination length. To keep the time continuity of the received symbols for the effective energy accumulation, we only consider the overlapping factor α between any two adjacent combination periods as shown in Fig. 3, i.e.,

$$\boldsymbol{X}_t\left((1-\alpha)l_{\rm sub}+1 : l_{\rm sub}\right) = \boldsymbol{X}_{t+1}(1 : \alpha l_{\rm sub}) \tag{38}$$

which implies that the tth combination period's "tail" is overlapped with the $(t+1)$th combination period's "head".

In the overlapping SRC algorithm, each combination period contains some received symbols that are commonly occupied by its two adjacent combination periods. This means three combination periods are partially overlapped with each other, which is also the essence of the overlapping SRC algorithm.

Let $\boldsymbol{X}_1 = [\boldsymbol{x}^{[1]}, \ldots, \boldsymbol{x}^{[l_{\rm sub}]}]$ denote the received symbol set in the first combination period. From (38), we can obtain $\boldsymbol{X}_t$ for the tth $(t = 2$ or $t = 3)$ combination period, where the ith element $\boldsymbol{X}_{t,i}$ of $\boldsymbol{X}_t$ can be derived as follows:

$$\boldsymbol{X}_{t,i} = \boldsymbol{x}^{[(t-1)(1-\alpha)l_{\rm sub}+i]}, \qquad \text{for} \quad 1 \le i \le l_{\rm sub}. \tag{39}$$

For three successive combination periods, there are a total of $2\alpha l_{\rm sub}$ received symbols commonly occupied, which means that combination length $l_{\rm sub}$ needs to be chosen such that

$$l_{\rm sub} = \frac{L}{3-2\alpha}. \tag{40}$$

In one combination period, the output SNR is the concave function of the combination length $l_{\rm sub}$, and the optimal solution $L_{\rm opt}$ under the large acceleration f_a is very small. Then, $l_{\rm sub} > L_{\rm opt}$ implies not only the decrease in the acquisition probability but also the waste of received symbols (i.e., a longer acquisition time). Hence, the combination length $l_{\rm sub}$ should be required to satisfy $l_{\rm sub} \le L_{\rm opt}$, i.e., the overlapping factor α should be chosen such that

$$\alpha \le 1.5 - \frac{L}{2L_{\rm opt}}. \tag{41}$$

Then, combined with the inherent restriction condition $0 \le \alpha \le 1$ that can be easily derived from Definition 1, (41) can be further rewritten as follows:

$$\begin{cases} 0 \le \alpha \le 1, & \text{if} \quad L \le L_{\rm opt} \\ 0 \le \alpha \le 1.5 - 0.5L/L_{\rm opt}, & \text{if} \quad L_{\rm opt} < L < 3L_{\rm opt} \\ \alpha = 0, & \text{if} \quad L \ge 3L_{\rm opt}. \end{cases} \tag{42}$$

From (42), we can observe that 1) if $L \ge 3L_{\rm opt}$, then $\alpha = 0$ is the unique solution; and 2) if $L < L_{\rm opt}$, then the solutions of α

TABLE I
MULTIPLE TYPICAL OVERLAPPING SCHEMES

L	α	$l_{\rm sub}$
$L_{\rm opt}$	0	$L_{\rm opt}/3$
	0.25	$0.4L_{\rm opt}$
	0.5	$0.5L_{\rm opt}$
	0.75	$2L_{\rm opt}/3$
	1.0	$L_{\rm opt}$
$2L_{\rm opt}$	0	$2L_{\rm opt}/3$
	0.25	$0.8L_{\rm opt}$
	0.5	$L_{\rm opt}$
$3L_{\rm opt}$	0	$L_{\rm opt}$

are not unique and lead to multiple overlapping schemes. For example, if $L = 2L_{\rm opt}$, we can choose either $\alpha = 0.5, l_{\rm sub} = L_{\rm opt}$, or $\alpha = 0, l_{\rm sub} = 2L_{\rm opt}/3$, or others. Furthermore, multiple typical overlapping schemes are presented in Table I.

In the overlapping SRC algorithm, the combination result $\boldsymbol{I}_{\rm oc}^{[t]}$ $(1 \le t \le 3)$ in the tth combination period can be derived as

$$\boldsymbol{I}_{\rm oc}^{[t]} = \sum_{i=1+(t-1)(1-\alpha)l_{\rm sub}}^{tl_{\rm sub}-(t-1)\alpha l_{\rm sub}} |\boldsymbol{I}^{[i]}|. \tag{43}$$

For $t = 1$ and $t = 2$, by substituting $\boldsymbol{I}_{\rm oc}^{[t]}$ and R into (7) and (8) respectively, we can obtain the acquisition results $\{\widehat{f}_d(1), \widehat{f}_d(2)\}$ in the first two combination periods.

Correspondingly, the SRC strategy shown in (11) needs to be modified for the overlapping SRC algorithm as follows:

$$\widetilde{R} = \Big[\max\{\widehat{f}_{\rm min} - 2\delta_{\rm oc} - 2\theta, -F_{\rm max}\} \quad \min\{\widehat{f}_{\rm max} + 2\delta_{\rm oc} + 2\theta, F_{\rm max}\}\Big] \tag{44}$$

where $\widehat{f}_{\rm min} = \min\{\widehat{f}_d(1), \widehat{f}_d(2)\}$, $\widehat{f}_{\rm max} = \max\{\widehat{f}_d(1), \widehat{f}_d(2)\}$, and $\delta_{\rm oc} = (1-\alpha)l_{\rm sub}\delta_s$ is the equivalent drift of Doppler shift during one combination period. Substituting $\boldsymbol{I}_{\rm oc}^{[3]}$ and this new search range $\widetilde{R}$ into (7) and (8), respectively, we can obtain the acquisition result $\widehat{f}_{\widetilde{d}}(3)$.

Next, we simply analyze the impact of overlapping factor on the acquisition probability. From (40), we can observe that $\partial l_{\rm sub}/\partial\alpha > 0$, which means that the combination length $l_{\rm sub}$ $(0 < l_{\rm sub} \le L_{\rm opt})$ monotonically increases as the overlapping factor α increases. For $0 < l_{\rm sub} \le L_{\rm opt}$, the output SNR is monotonically increasing with the combination length $l_{\rm sub}$ [16]. From the discussions earlier, we can derive that the larger overlapping factor α causes the larger combination length $l_{\rm sub}$ and further leads to the higher acquisition probability, under the constant L $(L \le 3L_{\rm opt})$ received symbols.

As compared with the single SRC algorithm, on one hand, the overlapping SRC algorithm has multiple choices of combination length and increases much flexibility of implementation, on the other hand, the overlapping SRC algorithm requires much less received symbols, thus saving much acquisition time, particularly under $L < 3L_{\rm opt}$. Clearly, if $\alpha = 0$ and $l_{\rm sub} = L_{\rm opt}$, the overlapping SRC algorithm degrades into the single SRC algorithm.

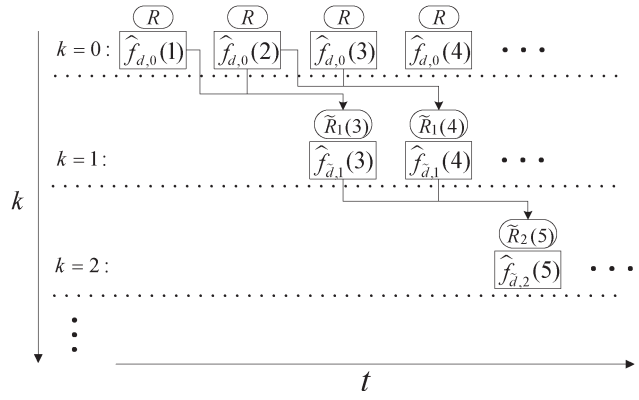

Fig. 4. Iterative SRC algorithm.

C. Iterative SRC Algorithm

The overlapping SRC algorithm uses three overlapping combination periods to correct the search range at the cost of less received symbols, as compared with the single SRC algorithm. However, the acquisition probability of Doppler shift cannot be further enhanced, although there are much more received symbols available (i.e., $L > 3L_{\rm opt}$). To overcome this shortage, we adopt the iterative of the overlapping SRC algorithm to further increase the acquisition probability, thus forming the iterative SRC algorithm that is described in Fig. 4.

Let k $(k \ge 0)$ denote the iteration step number and $\widehat{f}_{\widetilde{d},k}(t)$ denote the acquisition result derived in the tth combination period at the kth iteration step. In the iterative SRC algorithm, search range $\widetilde{R}_{k+1}(t)$ for the acquisition result $\widehat{f}_{\widetilde{d},k+1}(t)$ at the $(k+1)$th iteration step is determined by the acquisition results (i.e., $\{\widehat{f}_{\widetilde{d},k}(t-1), \widehat{f}_{\widetilde{d},k}(t)\}$) obtained at the kth iteration step. On the other hand, the acquisition results $\{\widehat{f}_{\widetilde{d},k+1}(t), \widehat{f}_{\widetilde{d},k+1}(t+1)\}$ at the $(k+1)$th iteration step determine the search range $\widetilde{R}_{k+2}(t+2)$ for the acquisition result $\widehat{f}_{\widetilde{d},k+2}(t+2)$ at the $(k+2)$th iteration step.

In Fig. 4, we can clearly observe that every iteration step requires two combination periods, which implies that the initial acquisition time at the kth iteration step starts at the $(2k+1)$th combination period. In addition to the first combination period, every combination period requires extra $(1-\alpha)l_{\rm sub}$ symbols. Let $T_{\rm total}$ and $K_{\rm total}$ denote the total number of combination periods and iteration steps, respectively, under L received symbols. Then, $T_{\rm total}$ and $K_{\rm total}$ are given by

$$T_{\rm total} = \left\lfloor 1 + \frac{L - l_{\rm sub}}{(1-\alpha)l_{\rm sub}} \right\rfloor \tag{45}$$

$$K_{\rm total} = \left\lfloor \frac{T_{\rm total} - 1}{2} \right\rfloor \tag{46}$$

where $\lfloor\zeta\rfloor$ denotes the largest integer less than or equal to ζ.

Therefore, we give the iterative SRC algorithm as follows:

Algorithm The Iterative SRC Algorithm

1) Received L ($L \geq 3L_{\text{opt}}$) symbols;
2) Set $t = 1$ and compute T_{total} according to (45);
3) **While** ($t \leq T_{\text{total}}$)
4) Compute $\boldsymbol{I}_{\text{oc}}^{[t]}$ according to (43);
5) Set $k = 0$ and $K = \lfloor (t-1)/2 \rfloor$, where K ($K \leq K_{\text{total}}$) denotes the iteration steps constructed by t combination periods;
6) **While** ($k \leq K$)
7) **If** $k = 0$
Compute $\widehat{f}_{d,k}(t)$ by substituting $\boldsymbol{I}_{\text{oc}}^{[t]}$ and R into (7) and (8), respectively;
8) **Else if** $k \geq 1$
Compute $\widehat{f}_{\widetilde{d},k}(t)$ by substituting $\boldsymbol{I}_{\text{oc}}^{[t]}$ and $\widetilde{R}_k(t)$ into (7) and (8), respectively, where

$$\begin{cases} \widetilde{R}_k(t) = \left[\max\left\{\widehat{f}_{\min}^{[k]} - 2\delta_{\text{oc}} - 2\theta, -F_{\max}\right\} \right. \\ \qquad\qquad \left. \min\left\{\widehat{f}_{\max}^{[k]} + 2\delta_{\text{oc}} + 2\theta, F_{\max}\right\}\right] \\ \widehat{f}_{\min}^{[k]} = \min\left\{\widehat{f}_{\widetilde{d},k-1}(t-2), \widehat{f}_{\widetilde{d},k-1}(t-1)\right\} \\ \widehat{f}_{\max}^{[k]} = \max\left\{\widehat{f}_{\widetilde{d},k-1}(t-2), \widehat{f}_{\widetilde{d},k-1}(t-1)\right\} \end{cases}. \quad (47)$$

9) **End if**
10) $k = k + 1$;
11) **End while**
12) $t = t + 1$;
13) **End while**
14) $\widehat{f}_{\widetilde{d},K_{\text{total}}}(2K_{\text{total}}+1)$ is the final acquisition result.

Let $\widetilde{p}_k$ denote the acquisition probability at the kth iteration step. From (36), we have

$$\widetilde{p}_k \geq \widetilde{p}_{k-1} \cdots \geq \widetilde{p}_0 = p. \quad (48)$$

Furthermore, we need to establish that the acquisition probability $\widetilde{p}_k$ approaches to 1. Next, we derive the upper bound, which is denoted by p^{ub}, for the acquisition probability $\widetilde{p}_k$ ($k \to \infty$). From Theorem 1, the search range $\widetilde{R}_k(2k+1)$ for $\widehat{f}_{\widetilde{d},k}(2k+1)$ iteratively falls into a more accurate search range with iteration step k as follows:

$$f_d(2k+1) \in \widetilde{R}_k(2k+1) \subseteq \cdots \subseteq \widetilde{R}_1(2k+1) \subseteq R. \quad (49)$$

Let $\widetilde{D}^{[k]}$ denote the length of the search range $\widetilde{R}_k(2k+1)$. From the proof of Theorem 2, we have

$$\widetilde{p}_k \leq p^{\frac{\widetilde{D}^{[k]} - 2\theta}{2F_{\max} - 2\theta}} \quad (50)$$

which monotonically decreases as $\widetilde{D}^{[k]}$ increases.

According to (47), the search range $\widetilde{R}_k(2k+1)$ is determined by the previous two acquisition results at the $(k-1)$th iteration step, i.e., $\widehat{f}_{\widetilde{d},k-1}(2k-1)$ and $\widehat{f}_{\widetilde{d},k-1}(2k)$. If and only if $\widehat{f}_{\widetilde{d},k-1}(2k-1) = f_d(2k-1)$ and $\widehat{f}_{\widetilde{d},k-1}(2k) = f_d(2k)$ (i.e., perfect acquisitions), there exists the minimum value, which is denoted by $\widetilde{D}_{\min}$, for $\widetilde{D}^{[k]}$, i.e.,

$$\begin{aligned} \widetilde{D}^{[k]} &\geq f_d(2k) + 2\delta_{\text{oc}} + 2\theta - (f_d(2k-1) - 2\delta_{\text{oc}} - 2\theta) \\ &= 5\delta_{\text{oc}} + 4\theta = \widetilde{D}_{\min}. \end{aligned} \quad (51)$$

By substituting (51) into (50), we can obtain p^{ub} as

$$\widetilde{p}_k \leq p^{\frac{\widetilde{D}_{\min} - 2\theta}{2F_{\max} - 2\theta}} = p^{\frac{5\delta_{\text{oc}} + 2\theta}{2F_{\max} - 2\theta}} = p^{\text{ub}}. \quad (52)$$

Under a high SNR scenario, the acquisition probability p is already very high. Then, by the single SRC algorithm, the acquisition probability $\widetilde{p}$, which is equivalent to $\widetilde{p}_1$ in the iterative SRC algorithm, even approaches closely to the upper bound p^{ub}. This means that the iterative SRC algorithm ($k \geq 2$) nearly provides no benefit, as compared with the single SRC algorithm. The value of SNR corresponding to the acquisition probability p in this case is the threshold above which the iterative SRC ($k \geq 2$) provides no benefit.

By the derivation of p^{ub} specified in (52) with respect to α, we can obtain

$$\frac{\partial p^{\text{ub}}}{\partial \alpha} = -\frac{5 l_{\text{sub}} \delta_{\text{s}} p^{\text{ub}} \ln p}{2F_{\max} - 2\theta} > 0 \quad (53)$$

which means that the iterative SRC algorithm with a larger overlapping factor α can provide a higher upper bound p^{ub}. It can also be explained that a larger α can confine the acquisition into a more accurate search range than a smaller α. Then, the required number of the received symbols at the kth iteration step, which is denoted by L_{req}^k, is given by

$$L_{\text{req}}^k = [1 + 2k(1-\alpha)]\, l_{\text{sub}} \quad (54)$$

which implies that a larger iteration step k and a smaller overlapping factor α result into a larger required number L_{req}^k. By rewriting (54), we can obtain

$$k = \frac{L_{\text{req}}^k - l_{\text{sub}}}{2(1-\alpha) l_{\text{sub}}} \quad (55)$$

which monotonically increases as α increases, due to $\partial k / \partial \alpha > 0$. In other words, for the constant number of symbols, a larger overlapping factor leads to a larger iteration step.

Then, we simply analyze the computational complexity for the proposed SRC scheme. Based on the radix-2 butterfly processing for FFT [31], the computational complexity for one single FFT includes $0.5 N_f \log_2 N_f$ complex multiplications and $N_f \log_2 N_f$ complex adders. In addition, the computational complexity for the noncoherent combination and spectrum peak search are $l_{\text{sub}} N_f$ and N_f complex adders, respectively. Therefore, we give the computational complexity for the single SRC, overlapping SRC, and iterative SRC algorithms in Table II.

In Table II, we can observe that the computational complexity is monotonically increasing with the required symbol number L_{req}^k and the iteration step k, respectively. From (53)–(55), we can derive that the overlapping factor α has a significant impact on the required symbol number L_{req}^k and the iteration step k. On one hand, for the constant k, a larger α corresponds to a smaller L_{req}^k. On the other hand, for the constant L_{req}^k, a

TABLE II
COMPUTATIONAL COMPLEXITY FOR THREE ALGORITHMS

algorithm	complex multiplications	complex adders
Single SRC	$1.5L_{\rm opt}N_f\log_2 N_f$	$3N_f(L_{\rm opt}\log_2 N_f + L_{\rm opt}+1)$
Overlapping SRC	$(1.5-\alpha)l_{\rm sub}N_f\log_2 N_f$	$2N_f[(1.5-\alpha)l_{\rm sub}\log_2 N_f + l_{\rm sub}+1]$
Iterative SRC	$0.5L^k_{\rm req}N_f\log_2 N_f$	$N_f[L^k_{\rm req}\log_2 N_f + (2k+1)(l_{\rm sub}+1)]$

TABLE III
SIMULATION PARAMETERS

Parameter	Value
Spread code rate	10.24 MHz
Spread code length	1024
Carrier frequency f_c	30.0 GHz
Relative velocity $v_{\max}$	12.0 km/s
Relative acceleration v_a	60×9.8 m/s^2
Sampling frequency f_s	20.48 MHz
Doppler-shift $F_{\max}$	1.2 MHz
Acceleration f_a	58.8 kHz/s
Symbol bit rate r_b	10.0 kb/s
Initial phase φ_0	0
FFT point N_f	2048
Tolerable threshold θ	20.0 kHz
SNR	$[-40,-33]$ dB

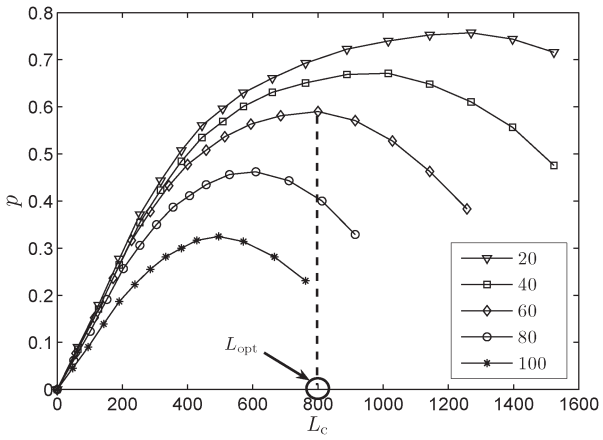

Fig. 5. Acquisition probability p versus L_c under different v_a ($\times$ 9.8 m/s^2).

larger α corresponds to a larger k. Hence, the iterative SRC algorithm obtains the significantly higher acquisition probability at the cost of higher computational complexity, as compared with the overlapping SRC and single SRC algorithms.

Clearly, the iterative SRC algorithm degrades into the overlapping SRC algorithm under $k=1$ and further degrades into the single SRC algorithm under $k=1$, $\alpha=0$, and $l_{\rm sub}=L_{\rm opt}$.

IV. SIMULATION RESULTS AND ANALYSIS

To evaluate the acquisition performance of our proposed SRC-based acquisition scheme, we adopt the DSSS system modulated on the Ka-band for the space communications [32]. Here, all the basic simulation parameters between the highly moving transmitter–receiver pair are set in Table III.

Fig. 5 plots the acquisition probability p versus the combination length L_c under different v_a. In Fig. 5, we can observe that p is the concave function with respect to L_c. As L_c increases, the acquisition probability p increases. However, once

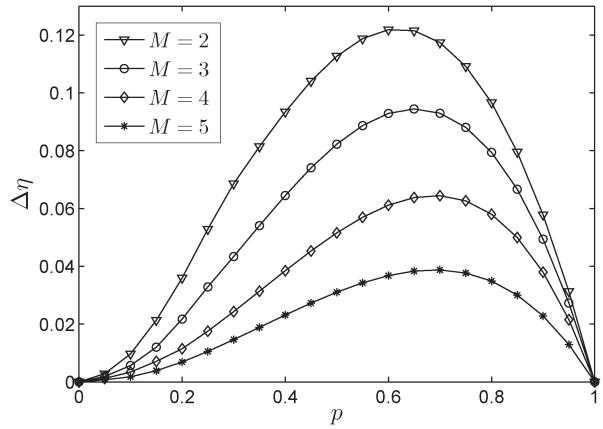

Fig. 6. Net increment $\triangle\eta$ versus p under different M.

the combination length L_c exceeds the optimal solution $L_{\rm opt}$, p decreases with L_c. Moreover, the optimal combination length $L_{\rm opt}$ is shown to monotonically decrease with the acceleration v_a. The large acceleration leads to the highly dynamic Doppler shift, which varies fast with the time, thus significantly dispersing the signal energy accumulation during the combination stage specified in (4). Moreover, this kind of serious energy dispersion problem severely decreases the output SNR, thus leading to a very low acquisition probability. For example, under $v_a = 20\times 9.8$ m/s^2, we can obtain the highest value of p as 0.75, whereas under $v_a = 100\times 9.8$ m/s^2, we only obtain the highest value of p as 0.32. Hence, we can observe that the large acceleration causes the serious energy dispersion problem, thus deteriorating the acquisition probability.

Fig. 6 gives the net increment $\triangle\eta$ versus the acquisition probability p under different values of M. Under any value of M, the net increment $\triangle\eta$ varies as the concave function with respective to the acquisition probability p and approaches to 0 if $p\to 0$ or $p\to 1$. For example, under $M=2$, $\triangle\eta$ first starts from 0 ($p=0$), then increases to its maximum value 0.12 ($p=0.60$), and finally decreases to 0 ($p=1$). Moreover, at the constant p, the net increment $\triangle\eta$ is monotonically decreasing with the value of M, which also coincides with the conclusions derived in (37). For example, at $p=0.60$, we can observe that $\triangle\eta = 0.12$, 0.09, 0.06, and 0.04 for $M=2$, 3, 4, and 5, respectively. Under the large acceleration scenario, the single SRC algorithm not only increases the acquisition probability but also shows the optimal number of combination periods.

Fig. 7 shows the acquisition probability $\widetilde{p}$ (i.e., $\widetilde{p}=p+\Delta\eta$) versus SNR under different M to evaluate the single SRC algorithm. Clearly, the time–frequency scheme in [17] only works well under the high SNR and then the acquisition probability dramatically decreases as the SNR decreases. The scheme proposed in [16] studies the impact of acceleration on output

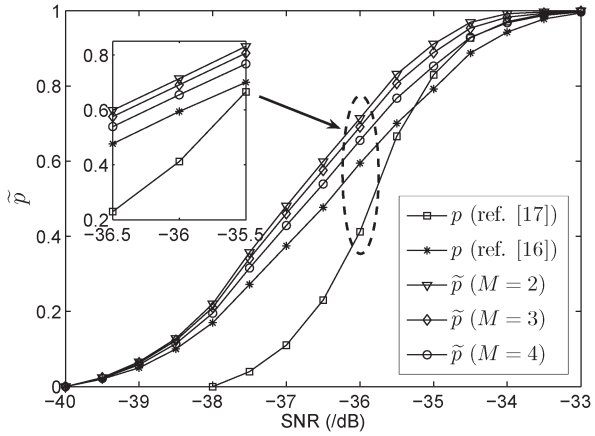

Fig. 7. Acquisition probability $\widetilde{p}$ versus SNR under different M.

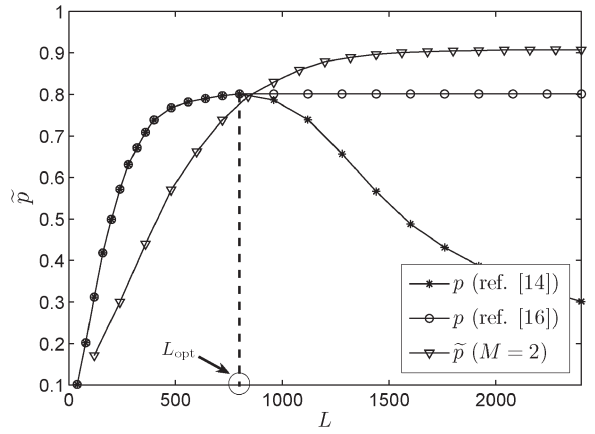

Fig. 8. Acquisition probability $\widetilde{p}$ versus L (SNR $= -35$ dB).

SNR. However, due to the serious energy dispersion problem, it can only get the very low acquisition probability. In this paper, we obtain the acquisition probability $\widetilde{p}$, which is higher for different values of M. For example, at SNR $= -36$ dB, the acquisition probability increases from $p = 0.59$ to $\widetilde{p} = 0.71$ $(M = 2)$, $\widetilde{p} = 0.68$ $(M = 3)$, and $\widetilde{p} = 0.65$ $(M = 4)$. On the other hand, we can observe that the net increment of acquisition probability is $\triangle\eta = 0.12$, 0.09, and 0.06 for $M = 2$, 3, and 4, respectively, which also coincides with the results in Fig. 6.

Fig. 8 presents the advantage of the SRC scheme over the scheme in [14] and the scheme in [16] at SNR $= -35$ dB. In the scheme proposed in [14], all the received symbols are directly combined in one combination period [i.e., $L_c = L$ in (4)], resulting in the serious energy dispersion problem and the very low acquisition probability. Hence, the acquisition probability is a concave function with the symbol number L, and the optimal length is $L_{\rm opt} = 800$, which also agrees with the results in Fig. 5. In the scheme [16], the combination length $L_c = L_{\rm opt}$ if $L \geq L_{\rm opt}$. This means more received symbols are not beneficial for the acquisition performance. In the SRC scheme, we split all the received symbols equally into three periods (i.e., $L_c = L/3$). As compared with p derived in schemes [14] and [16], the acquisition probability $\widetilde{p}$ is higher as long as $L > 900$, i.e., our proposed SRC scheme can effectively increase the acquisition probability by exploiting all the received symbols available.

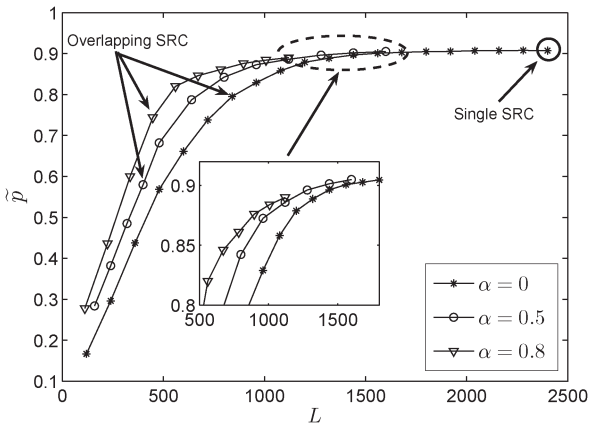

Fig. 9. Acquisition probability $\widetilde{p}$ versus L $(L \leq 3L_{\rm opt})$ under different α (SNR $= -35$ dB).

Fig. 9 evaluates the overlapping factor's impact on the acquisition probability at SNR $= -35$ dB, using the overlapping SRC algorithm. For some value of L, there are multiple choices for α. Moreover, a smaller L covers a wider range for the solution to α, which is determined by the restriction condition derived in (42). Under $L = 3L_{\rm opt} = 2400$ and $\alpha = 0$, the overlapping SRC algorithm degrades into the single SRC algorithm. It indicates the single SRC algorithm is an extreme case of the overlapping SRC algorithm. The acquisition probability for the single SRC algorithm is 0.912, at the cost of 2400 symbols. However, the overlapping SRC algorithm, which uses much fewer symbols, can achieve the acquisition probability slightly lower than 0.912. For example, under $\alpha = 0.8$ and $l_{\rm sub} = L_{\rm opt}$, the overlapping SRC algorithm achieves the acquisition probability of 0.89 using only $(3 - 2\alpha)L_{\rm opt} = 1120$ symbols. Furthermore, for the constant L, the overlapping SRC algorithm under a larger α can achieve the higher acquisition probability than that under a smaller α. For example, at $L = 1000$, the acquisition probability is $\widetilde{p} = 0.83$, 0.87, and 0.88 for $\alpha = 0$, 0.5, and 0.8, respectively. This is because a smaller overlapping factor α brings a longer combination length $l_{\rm sub}$, which is given in (40). On one hand, the overlapping SRC algorithm can nearly achieve the acquisition probability as high as the single SRC algorithm at the cost of far fewer symbols. On the other hand, the overlapping SRC algorithm can obtain the higher acquisition probability under a larger overlapping factor than that under a smaller overlapping factor.

Fig. 10 plots the acquisition probability $\widetilde{p}_k$ versus the iteration step k, using three SRC algorithms. As compared with the overlapping SRC algorithm, the iterative SRC algorithm obtains a significant increase in acquisition probability. For example, under $\alpha = 0$ and SNR $= -36$ dB, the acquisition probability $\widetilde{p}_k$ starts from 0.59 (i.e., the acquisition probability p derived by the scheme [16]) and it increases up to 0.71 (i.e., the acquisition probability $\widetilde{p}$ derived by the single SRC algorithm). Then, with the iteration step k, $\widetilde{p}_k$ continually increases to 0.75, $0.78, \ldots$ and finally becomes stable at about 0.86. The similar variation of $\widetilde{p}_k$ with k also happens for $\alpha = 0.5$. Under the large acceleration scenario, the iterative SRC algorithm significantly increases the acquisition probability. In other words, the iterative SRC greatly mitigates the energy dispersion problem by narrowing the search range for Doppler shift acquisition.

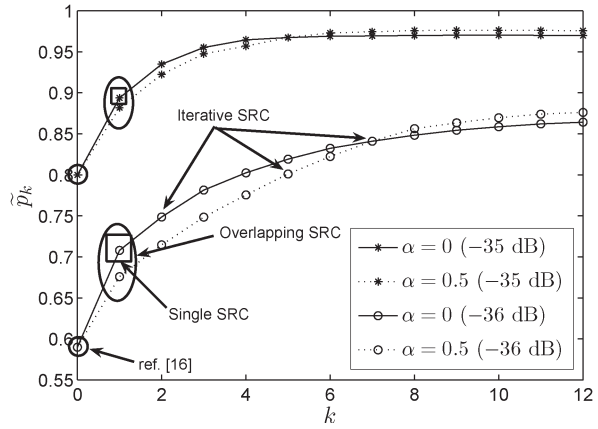

Fig. 10. Acquisition probability $\widetilde{p}_k$ versus the iteration step k under three SRC algorithms.

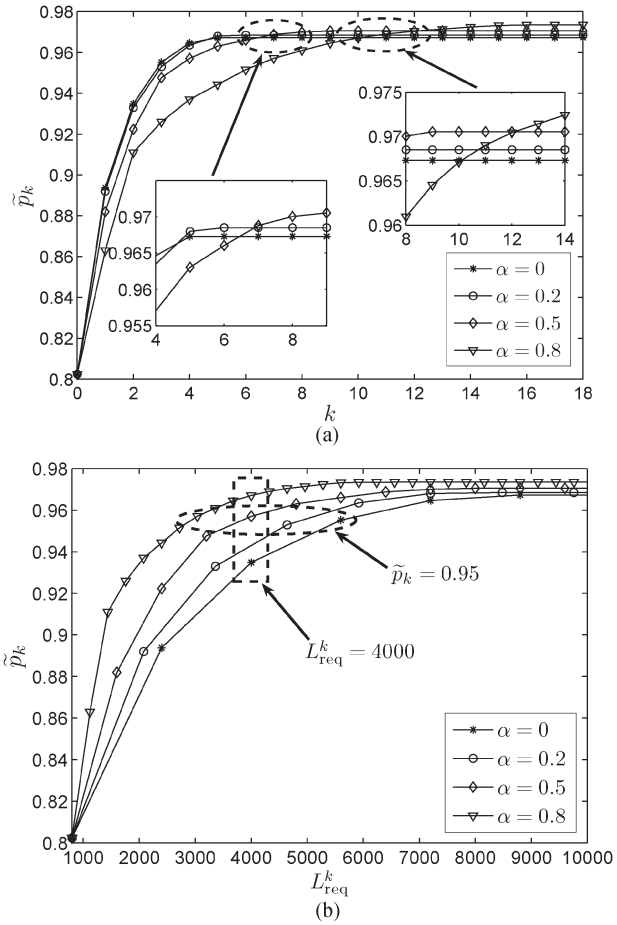

Fig. 11. Acquisition probability $\widetilde{p}_k$ versus k and $L^k_{\rm req}$, respectively, under different α (SNR $= -35$ dB).

Fig. 11 gives the acquisition probability $\widetilde{p}_k$ versus the iteration step k and the required symbol number $L^k_{\rm req}$, respectively, using the iterative SRC algorithm. Under $\alpha = 0$, 0.2, 0.5, and 0.8, the acquisition probability $\widetilde{p}_k$ starts from 0.80 and continually increases with the iteration step k. In Fig. 11(a), under a larger α, $\widetilde{p}_k$ grows slower with k but eventually converges to a higher value than that under a smaller α. For example, $\widetilde{p}_k$ $(\alpha = 0.2)$ exceeds $\widetilde{p}_k$ $(\alpha = 0)$ at $k = 5$, $\widetilde{p}_k$ $(\alpha = 0.5)$ exceeds $\widetilde{p}_k$ $(\alpha = 0.2)$ at $k = 7$, and $\widetilde{p}_k$ $(\alpha = 0.8)$ exceeds $\widetilde{p}_k$ $(\alpha = 0.5)$ at $k = 12$. From the perspective of $L^k_{\rm req}$, we show the relationship between $\widetilde{p}_k$ and $L^k_{\rm req}$ in Fig. 11(b), based on the transformation given by (55). We can find that, for the constant acquisition probability $\widetilde{p}_k$, a larger overlapping factor α corresponds to a smaller number $L^k_{\rm req}$ of received symbols. For example, for $\widetilde{p}_k = 0.95$, the required number of symbols is $L^k_{\rm req} = 5600$, 4640, 4000, and 3040 under $\alpha = 0$, 0.2, 0.5, and 0.8, at the iteration step $k = 3$, 3, 4, and 7, respectively, Clearly, $\alpha = 0.8$ saves 2560 symbols as compared with $\alpha = 0$. For $L^k_{\rm req} = 4000$, the acquisition probability is $\widetilde{p}_k = 0.935$ $(k = 2)$, 0.956 $(k = 4)$, and 0.965 $(k = 10)$ under $\alpha = 0$, 0.5, and 0.8, respectively. However, $\alpha = 0.5$ and $\alpha = 0.8$ require extra 6.56×10^6 and 26.24×10^6 adders, respectively, as compared with $\alpha = 0$. From the discussions in Fig. 11(a) and (b), we can find that, under the larger overlapping factor, the iterative SRC algorithm achieves the higher acquisition probability with far fewer symbols at the cost of higher computational complexity.

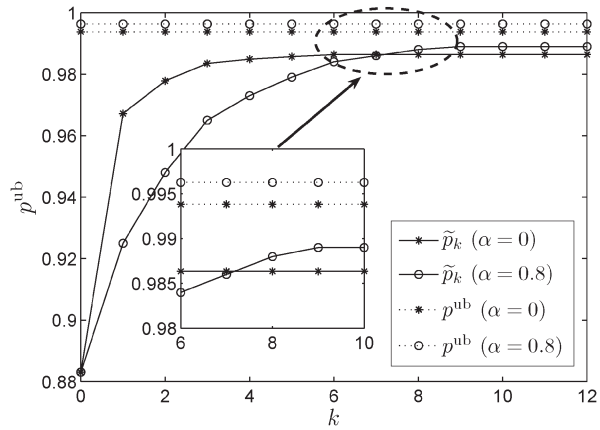

Fig. 12. Upper bound $p^{\rm ub}$ versus k under different α (SNR $= -34.5$ dB).

Fig. 12 shows the upper bound $p^{\rm ub}$ versus the iteration step k at SNR $= -34.5$ dB. The acquisition probability $\widetilde{p}_k$ always starts from $\widetilde{p}_0 = p = 0.884$ and then continually increases until converges to one constant value. Moreover, the constant value is slightly lower than the theoretical upper bound $p^{\rm ub}$ given by (52). For example, under $\alpha = 0$, $\widetilde{p}_k$ increases and eventually converges to 0.987, whereas its corresponding theoretical upper bound is $p^{\rm ub} = 0.994$. Under $\alpha = 0.8$, $\widetilde{p}_k$ increases and eventually converges to 0.989, whereas its corresponding theoretical upper bound is $p^{\rm ub} = 0.996$. The comparison between $\alpha = 0$ and $\alpha = 0.8$ shows that the upper bound $p^{\rm ub}$ under a larger α is higher than that under a smaller α, which also verifies the conclusions derived in (53).

Fig. 13 shows the variation of acquisition bias with the iteration step k at SNR $= -34$ dB. In Fig. 13(a) $(k = 0)$, we can observe that the number of acquisition bias larger than the tolerable threshold is very great, nearly 80 in 1000 times simulations. This means the acquisition probability is 0.92. In addition, the amplitude of acquisition bias is very large and varies from -2.4 to 2.4 MHz. The large acceleration results in the highly dynamic Doppler shift, which drifts over a very wide frequency range. However, as shown in Fig. 13(b) $(k = 3)$, the acquisition bias is reduced to a much smaller range ([−15, 15] kHz), which implies that the acquisition probability

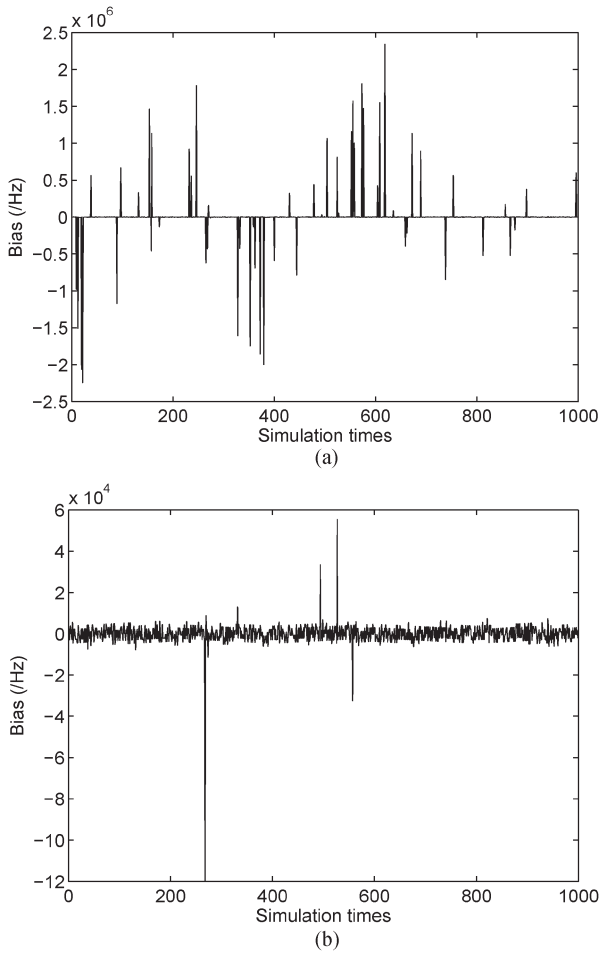

Fig. 13. Acquisition bias at different k using the iterative SRC algorithm.

approaches to 1. In other words, the SRC scheme significantly confines the Doppler shift acquisition into a more accurate search range, thus significantly decreasing the acquisition bias. As shown in Fig. 13, using the iterative SRC algorithm, we can significantly reduce the acquisition bias of Doppler shift both in number and amplitude.

V. Conclusion

To address the Doppler shift acquisition problem not only under a very low SNR but also under very large acceleration for space communications, we develop the SRC-based acquisition scheme, including three algorithms to significantly improve the acquisition performance. First, we show that the single SRC algorithm can increase the acquisition probability by narrowing the search range for spectrum peak search. Second, the overlapping SRC algorithm, which is based on the overlapping of single SRC algorithm, is shown to not only increase the implementation flexibility but to achieve the high acquisition probability with far fewer symbols as well. Third, the iterative SRC algorithm, which builds on the iterative of overlapping SRC algorithm, can obtain the highest acquisition probability closest to its theoretical upper bound. By the analyses and simulations, we show that the developed SRC scheme can significantly increase the acquisition probability for space communications.

References

[1] L. J. Ippolito, "Radio propagation for space communications systems," *Proc. IEEE*, vol. 69, no. 6, pp. 697–727, Jun. 1981.
[2] T. De Cola, E. Paolini, G. Liva, and G. P. Calzolari, "Reliability options for data communications in the future deep-space missions," *Proc. IEEE*, vol. 99, no. 11, pp. 2056–2074, Nov. 2011.
[3] P. D. Groves, *Principles of GNSS, Inertial, and Multisensor Integrated Navigation Systems*. Norwood, MA, USA: Artech House, 2013.
[4] R. A. Yingst, B. A. Cohen, D. W. Ming, and D. B. Eppler, "Comparing apollo and mars exploration rover (MER)/phoenix operations paradigms for human exploration during NASA Desert-RATS science operations," *Acta Astronautica*, vol. 90, no. 2, pp. 311–317, Oct. 2013.
[5] A. Wang, W. Dong, and Y. Shen, "The algorithm for deep-space weak signal tracking using a modified Kalman filter," in *Proc. IEEE Int. Conf. Wireless Commun., Netw. Mobile Comput.*, 2011, pp. 1–4.
[6] S. Kandeepan, "Steady state distribution of a hyperbolic digital tanlock loop with extended pull-in range for frequency synchronization in high Doppler environment," *IEEE Trans. Wireless Commun.*, vol. 8, no. 2, pp. 890–897, Feb. 2009.
[7] M. Erlihson, D. Ezri, Z. Hadad, and O. Shalem, "Method for Doppler Shift Estimation and Compensation in a Communications System," U.S. Patent 8 254 281, Aug. 28, 2012.
[8] T. Wang, C. Li, W. Meng, H.-H. Chen, and M. Guizani, "EM-based adaptive frequency domain estimation of Doppler shifts with CRLB analysis for CDMA systems," *IEEE Trans. Commun.*, vol. 60, no. 1, pp. 198–298, Jan. 2012.
[9] S. H. Kong, "A deterministic compressed GNSS acquisition technique," *IEEE Trans. Veh. Technol.*, vol. 62, no. 2, pp. 511–521, Feb. 2013.
[10] S. Amiri and M. Mehdipour, "Accurate Doppler frequency shift estimation for any satellite orbit," in *Proc. IEEE Int. Conf. Recent Adv. Space Technol.*, 2007, pp. 602–607.
[11] D. C. Rife and R. R. Boorstyn, "Single tone parameter estimation from discrete-time observations," *IEEE Trans. Inf. Theory*, vol. IT-20, no. 5, pp. 591–598, Sep. 1974.
[12] S. M. Spangenberg, I. Scott, and S. Mclaughlin, "An FFT-based approach for fast acquisition in spread spectrum communication systems," *Wireless Pers. Commun.*, vol. 13, no. 1/2, pp. 27–56, May 2000.
[13] D. Akopian, "Fast FFT based GPS satellite acquisition methods," *IEE Radar, Sonar Navigat.*, vol. 152, no. 4, pp. 277–286, Aug. 2005.
[14] D. Borio, C. O'Driscoll, and G. Lachapelle, "Coherent, noncoherent and differentially coherent combining techniques for acquisition of new composite GNSS signals," *IEEE Trans. Aerosp. Electron. Syst.*, vol. 45, no. 3, pp. 1227–1240, Jul. 2009.
[15] H. Elders-Boll and U. Dettmar, "Efficient differentially coherent code/Doppler acquisition of weak GPS signals," in *Proc. IEEE Int. Symp. Spread Spectrum Techn. Appl.*, 2004, pp. 731–735.
[16] A. Yasotharan and T. Thayaparan, "Strengths and limitations of the Fourier method for detecting accelerating targets by pulse Doppler radar," *Proc. Inst. Elect. Eng.—Radar, Sonar Navigat.*, vol. 149, no. 2, pp. 83–88, Apr. 2002.
[17] A. Yasotharan and T. Thayaparan, "Time-frequency method for detecting an accelerating target in sea clutter," *IEEE Trans. Aerosp. Electron. Syst.*, vol. 42, no. 4, pp. 1289–1310, Oct. 2006.
[18] J. W. Park and J. S. Won, "An efficient method of Doppler parameter estimation in the time-frequency domain for a moving object from TerraSAR-X data," *IEEE Trans. Geosci. Remote Sens.*, vol. 49, no. 12, pp. 4771–4787, Dec. 2011.
[19] B. S. Sharif, J. Neasham, O. R. Hinton, and A. E. Adams, "A computationally efficient Doppler compensation system for underwater acoustic communications," *IEEE J. Ocean. Eng.*, vol. 25, no. 1, pp. 52–61, Jan. 2000.
[20] P. W. Moo and Z. Ding, "Tracking performance of MIMO radar for accelerating targets," *IEEE Trans. Signal Process.*, vol. 61, no. 21, pp. 5205–5216, Nov. 2013.
[21] V. Vilnrotter, K. Andrews, J. Hamkins, and A. Tkacenko, "Maximum likelihood estimation of navigation parameters from downlink telemetry," in *Proc. IEEE Aerosp. Conf.*, 2010, pp. 1–9.
[22] Y. V. Zakharov, V. M. Baronkin, and T. C. Tozer, "DFT-based frequency estimators with narrow acquisition range," *Proc. Inst. Elect. Eng.—Commun.*, vol. 148, no. 1, pp. 1237–1242, Feb. 2001.
[23] C. Candan, "A method for fine resolution frequency estimation from three DFT samples," *IEEE Signal Process. Lett.*, vol. 18, no. 6, pp. 351–354, Jun. 2011.
[24] E. Aboutanios and B. Mulgrew, "Iterative frequency estimation by interpolation on Fourier coefficients," *IEEE Trans. Signal Process.*, vol. 53, no. 4, pp. 1237–1242, Apr. 2005.

[25] E. Aboutanios, "A modified dichotomous search frequency estimator," *IEEE Signal Process. Lett.*, vol. 11, no. 2, pp. 186–188, Feb. 2004.
[26] K.-J. Yang, C.-L. Wang, and Y.-R. Tsai, "Joint channel and Doppler spread estimation over time-varying flat fading channels," in *Proc. IEEE Veh. Technol. Conf. (Spring)*, 2012, pp. 1–5.
[27] Z. Zhang, Y. Li, and H. Zhang, "Error correction based Doppler estimation method for Doppler smearing," *Electron. Lett.*, vol. 49, no. 12, pp. 769–770, Jun. 2013.
[28] C. W. Helstrom, *Elements of Signal Detection and Estimation*. Englewood Cliffs, NJ, USA: Prentice-Hall, 1995.
[29] R. Durrett, *Probability: Theorem and Examples*. Cambridge, U.K.: Cambridge Univ. Press, 2010.
[30] S. P. Boyd and L. Vandenberghe, *Convex Optimization*. Cambridge, U.K.: Cambridge Univ. Press, 2004.
[31] P. Duhamel and H. Hollmann, "Split radix FFT algorithm," *Electron. Lett.*, vol. 20, no. 1, pp. 14–16, 1984.
[32] H. Hemmati *et al.*, "Comparative study of optical and radio-frequency communication systems for a deep-space mission," Jet Propulsion Lab., Pasadena, CA, USA, TDA Progress Rep. 42-128, 1997.

Zhaowei Zhang received the B.S. and Ph.D. degrees in telecommunication engineering from Xidian University, Xi'an, China, in 2009 and 2014, respectively.

He is currently with the State Key Laboratory of Integrated Service Networks, Xidian University. He is the author of several papers published in scientific journals, such as IEEE COMMUNICATIONS LETTERS and *IET Electronics Letters*, and has presented at several conferences, such as the IEEE Wireless Communications and Networking Conference. His research interests include signal processing, parameter estimation, and resource allocation in communications.

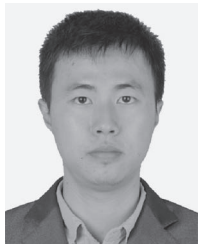

Wenchi Cheng (M'14) received the Ph.D. degree in telecommunication engineering from Xidian University, Xi'an, China.

From 2010 to 2011, he was a Visiting Ph.D. Student with the Networking and Information Systems Laboratory, Department of Electrical and Computer Engineering, Texas A&M University, College Station, TX, USA. Since 2013, he has been an Assistant Professor with Xidian University. His research interests include fifth-generation wireless networks, wireless full-duplex transmission, statistical quality-of-service provisioning, cognitive radio techniques, and energy-efficient wireless networks. He is the author of several papers published in several journals, such as the IEEE JOURNAL ON SELECTED AREAS IN COMMUNICATIONS, IEEE WIRELESS COMMUNICATIONS MAGAZINE, and IEEE NETWORK MAGAZINE, and he has presented at several conferences, such as the IEEE International Conference on Computer Communications (IEEE INFOCOM), the IEEE Global Communications Conference (IEEE GLOBECOM), and the IEEE International Conference on Communications (IEEE ICC).

Dr. Cheng is serving as a Technical Program Committee member for IEEE ICC 2015, IEEE GLOBECOM 2016, and IEEE INFOCOM 2016.

Hailin Zhang (M'98) received the B.S. and M.S. degrees from Northwestern Polytechnic University, Xi'an, China, in 1985 and 1988, respectively, and the Ph.D. degree from Xidian University, Xi'an, in 1991.

Since 1991, he has been with the School of Telecommunications Engineering, Xidian University, where he is currently a Senior Professor and the School Dean. He is also currently the Director of the Key Laboratory in Wireless Communications sponsored by the Chinese Ministry of Information Technology, a key member of the State Key Laboratory of Integrated Services Networks, one of the state government specially compensated scientists and engineers, a field leader in telecommunications and information systems at Xidian University, and an Associate Director for the National 111 Project. He is the author of more than 100 papers published in scientific journals and presented at conferences. His current research interests include key transmission technologies and standards on broadband wireless communications for fifth-generation wireless access systems.